

Title: Distinct Oscillation Dynamics Selectively Coordinate Excitatory and Inhibitory Neurons in Prefrontal Cortex during Sensory Discrimination

Hua-an Tseng and Xue Han

Biomedical Engineer Department, Boston University, Boston, MA, 02215

Correspondence: Xue Han (xuehan@bu.edu), Hua-an Tseng (hatseng@bu.edu)

Abstract

The prefrontal cortex (PFC) is crucial for many cognitive functions. PFC individual neuron activity and ensemble oscillation dynamics have been linked to unique aspects of behavior. However, it remains largely unclear how different neuron types relate to oscillation features. To understand how excitatory and inhibitory neurons in PFC are coordinated by distinct oscillation signatures, we designed a 3-choice auditory discrimination task and used tetrode devices to examine individual PFC neuron activity and ensemble LFP oscillations in task performing mice. We found that PFC neurons and ensemble LFP oscillations exhibited complex sensory evoked responses that are context and task-progression dependent. While both excitatory and inhibitory neurons were transiently modulated at different phases of the task, inhibitory neurons were increasingly recruited as trial progressed compared to excitatory neurons. Inhibitory neurons in general showed higher spike-field coherence with LFP oscillations than excitatory neurons throughout the task period, first at higher frequencies at the beginning of the task, and then transitioned to lower frequencies in the middle of the task that

sustained beyond task completion. Together, our results demonstrate that excitatory and inhibitory neurons selectively engage distinct oscillation dynamics during sensory discrimination in mice.

Introduction

The prefrontal cortex (PFC) is known to be critically involved in decision making, and damage to the PFC leads to deficits in various cognitive performance (Miller, 2000, Miller and Cohen, 2001, Dalley et al., 2004, Rossi et al., 2007, Gregoriou et al., 2014, Duan et al., 2015, Hanks and Summerfield, 2017). Goal-orientated decision making involves detecting sensory stimuli, applying learned rules, and executing an outcome. PFC activities—both individual neurons’ spiking patterns and population local field potential (LFP) oscillation dynamics—have been correlated with many aspects of decision making process, such as attention, sensory processing, rule utilization, working memory, task progression tracking, and result anticipation.

Recent studies using optogenetics to manipulate the activity of genetically defined cell types have showed that different PFC cell types are associated with distinct aspects of cognitive tasks (Hussar and Pasternak, 2009, Kvitsiani et al., 2013, Sparta et al., 2014, Murray et al., 2015, Kim et al., 2016a). In general, excitatory neurons participate in various aspects of a task, whereas different subtypes of inhibitory neurons seem to be preferentially recruited during different stages of a task. Calcium imaging of different PFC neuron subtypes in a go/no-go task further revealed that excitatory neurons exhibit heterogeneous responses, while inhibitory neuron activity tends to be more correlated within their subtypes (Pinto and Dan, 2015, Kim et al., 2016a, Kamigaki and Dan, 2017), presumably due to gap junction coupling (Gibson et al., 1999). Parvalbumin-expressing (PV) neurons were shown to respond to various aspect of a task (Pinto and Dan, 2015, Lagler et al., 2016), especially reward (Kvitsiani et al.,

2013, Sparta et al., 2014), whereas somatostatin-expressing (SST) neurons tend to be more selective and respond primarily to sensory stimuli and motor activity (Kvitsiani et al., 2013, Pinto and Dan, 2015).

LFP oscillations in the PFC have also been associated with distinct cognitive functions, and are coordinated with LFP oscillations in other cortical and subcortical areas. For example, theta oscillations (~5-10Hz), closely related to working memory (Liebe et al., 2012), can coordinate long range connections between the PFC and the hippocampus (Dejean et al., 2016). Beta oscillations (~15-30Hz), largely associated with status-quo and rule application (Buschman et al., 2012), are often synchronized over shorter distances, within the PFC, or between the PFC and other cortical areas. Higher frequency oscillations, such as gamma oscillations (~35-100Hz) are found to be involved in encoding/decoding of working memory (Lundqvist et al., 2016) and attention (Gregoriou et al., 2009).

It has been suggested that LFP oscillations may organize neurons into functional ensembles (Watrous et al., 2015, Helfrich and Knight, 2016). For example, spike-field coherence between the PFC and the sensory cortex was increased during covert attention (Gregoriou et al., 2009), and spike-field coherence within the sensory cortex was found to be correlated with behavioral performance (Womelsdorf et al., 2006). Recent optogenetic experiments showed that abnormal activity of inhibitory neurons can disrupt gamma oscillations and lead to cognitive deficiency, highlighting the power of transgenic mouse models in cell type-specific investigation of PFC neural networks (Cho et al., 2015). While much of our knowledge of the PFC has been obtained in humans, monkeys, and rats, much less is known about the PFC in mice, a model organism with advanced genetic tools that allow detailed examination of the functional significance of distinct neuron subtypes. Here we recorded both spikes and LFPs simultaneously in the PFC while mice were freely moving and performing a 3-choice auditory discrimination task. With tetrode devices, we were able to identify well-isolated individual PFC neurons and distinguish excitatory neurons from inhibitory neurons using waveform features. We found that mouse PFC neurons and LFP oscillations were modulated during the sensory discrimination task, as

observed in other animal models and humans. In addition, spike-field coherence was modulated across multiple frequency bands, in a behavioral stage- and cell type-dependent manner. Inhibitory neurons overall showed higher coherence with LFPs compared to excitatory neurons, which were significant first at gamma frequencies at the beginning of the task, then at theta and alpha frequency as trial progressed, and subsequently transitioned back to gamma frequencies towards trial completion.

Results

A large fraction of Mouse PFC neurons exhibited task related spiking activities

To understand how distinct cell types are recruited during sensory discrimination, we designed a 3-choice auditory discrimination task, which required freely moving mice to associate a specific auditory stimulus with a predefined “reward” location (Figure 1A). During the task, mice self-initiated each trial by stepping into the “initiation” location to trigger one of the three auditory cues (10 kHz sine wave, 25 click/second and 100 click/second), which was presented to the mice throughout the trial. After initiation, mice were given 5 seconds to reach the “reward” location on the other end of the arena to receive a reward (correct trial). If mice reached the other two incorrect “reward” locations (incorrect trial) or failed to reach any “reward” location within 5 seconds (incomplete trial, excluded in this study), they were presented with a 5-second timeout, with bright light illuminating all “reward” locations. Throughout the recording period, all mice regained and maintained a performance of >60% correct rate over the recording period (Figure 1B). Most mice were able to complete each trial within 3 seconds, with an averaged reaction time of 1.31 ± 0.57 seconds across all completed trials in 6 mice (Figure 1C). We performed a total of 251 recording sessions in 6 mice, in PFC bilaterally, and identified 711 single neurons based on simultaneously recorded waveforms from four closely positioned tetrode wires (Fig. 1D). Among these 711 neurons, 552 (78%) showed significant changes in their firing rates during the task

when compared to the inter-trial interval (ITI) ($p < 0.05$, Wilcoxon rank sum test). We excluded 159 (22%) neurons that were not modulated by the task from further analysis. Of the 552 task-relevant neurons, the width of their spike waveforms followed a bi-normal distribution (Fig. 1E) with one peak centered at 0.45 ms, consistent with the general observation of putative excitatory neurons (Figure 1 D1), and another peak centered at 0.25 ms, consistent with the general observation of putative inhibitory neurons (Figure 1 D2) (Cardin et al., 2007, Mitchell et al., 2007, Han et al., 2009, Lee et al., 2017). Thus, we further divided these neurons into putative excitatory neurons and putative inhibitory neurons based on their spiking width, using 0.4 ms as a threshold. We identified 441 excitatory neurons (80%) and 111 inhibitory neurons (20%). The recorded excitatory neurons exhibited a lower firing rate comparing to the inhibitory neurons (excitatory: 1.66 ± 1.84 Hz, inhibitory: 2.62 ± 2.68 Hz; $p < 0.05$, Wilcoxon Ranksum test).

Excitatory neurons and inhibitory neurons were preferentially modulated at different phases of the task

We first examined the timing of PFC spiking relative to the phase of a trial. When aligned to trial start, some neurons showed an immediate increase in firing rate centered at trial start upon sound onset (Figure 2A), some exhibited a delayed increase in firing in the middle of the trial (Figure 2B), and some increased firing at the end of the trial (Figure 2C). Given the variation in the time to complete each trial, we normalized the firing rate to task progression to track neural responses throughout the task. Indeed, firing rate were task progression-dependent, with increase in firing rates at different stages of the task (Figures 2A-C).

To compare responses of excitatory and inhibitory neurons, we first calculated the firing rates of each individual neuron, and then sorted them according to the timing when their firing rates peaked. As a

population, we found that both excitatory and inhibitory neurons were transiently modulated at different phases of the task (Figure 2D). Excitatory neurons tended to be modulated at the early stage of the task, whereas most inhibitory neurons were modulated towards the end of the task (Figure 3E; $p < 0.01$, χ^2 test). These results suggest that discrete PFC neuron subgroups are related to different aspects of sensory discrimination, and that excitatory and inhibitory neurons are recruited at different phases of the task.

The diverse temporal profiles, and the existence of delayed and transient activity throughout the task suggested that PFC responses were relevant to the discrimination task; however, an alternative explanation could be that they were driven primarily bottom up by auditory stimuli presented throughout the trial. To rule out the possibility that the PFC was solely driven by bottom up auditory stimuli, we designed a “passive listening” block, during which mice received the same auditory stimuli but without performing the discrimination task. Mice were placed in the same arena with a floor that covered the sensors at the “initiation” and “reward” locations. The “passive listening” block contained 200-250 trials. During each trial, one of the same three auditory stimuli was randomly presented for 1.5-3 seconds, followed by a 1.5-3 seconds long inter-trial interval (ITI). To compare the activity of the same neuron during discrimination task versus during passive listening, the “passive listening” block was performed either before or after the “discrimination task” in the same recording session.

Of the 552 task-modulated neurons, 422 neurons were also tested with the “passive listening” condition. Of these 422 neurons, only 12 (3%) neurons showed significant differences in firing rate when auditory stimuli were presented during passive listening ($p < 0.05$, Wilcoxon rank sum test). Neurons that were modulated during the task showed largely no response to auditory stimuli during passive listening (representative neurons shown in Figure 2). As a population, PFC neurons failed to produce any responses during the “passive listening” condition, confirming that PFC neurons exhibit task-specific modulation, rather than responding to bottom-up auditory stimuli alone (Figure 2D). While PFC neurons

are known to respond to auditory stimuli during passive conditions (Romanski and Goldman-Rakic, 2002, Miller et al., 2015), in our study, using the three auditory stimuli at ~70dB over an ambient environment of ~60dB, was not sufficient to evoke significant passive responses in the PFC.

We further examined whether PFC neurons responded differently according to task outcomes. We calculated the firing rates during correct and incorrect trials, and sorted the excitatory and inhibitory neurons based on their peak firing rates during correct trials. We found that both excitatory and inhibitory neurons showed clear sequential activity during the correct trials (Figure S1A), but not during the incorrect trials (Figure S1B), confirming that both excitatory and inhibitory neurons are modulated by task outcomes.

PFC neurons exhibited complex activation patterns during three stimuli discrimination, and inhibitory neurons were increasingly recruited as trial progressed.

While PFC neurons are broadly tuned to auditory stimuli, they are known to discriminate sensory stimuli, such as categorizing sensory inputs (Freedman et al., 2001, Miller and Cohen, 2001, Lee et al., 2009). To examine whether mouse PFC neurons are selectively modulated by different auditory cues or can discriminate different cues, we compared their responses to different auditory cues. We observed that PFC neurons exhibited highly heterogeneous responses when different cues were presented (Figure 3A and B). Some PFC neurons responded to only one auditory cue but not the other two (Figure 3A), whereas some responded to all cues but with distinct time course, i.e. small and transient response to one cue and robust and long lasting response to the other two (Figure 3B). This demonstrates that while some PFC neurons responded only to one specific cue, others may show complex and distinct response to different cues. It further suggests that when animals were required to distinguish more than two

cues, they were able to utilize the combination of neurons with various response amplitude and temporal kinetics, which may effectively expand their coding capacity.

To quantify the selectivity of each PFC neuron between different auditory cues at different phase of the task, we calculated the p -value (One-way ANOVA) between the firing rates during different auditory cues throughout trial progression. We found that many PFC neurons exhibited differential responses to the presentation of different auditory cues (Figure 3C). As a population, we found that the fraction of neurons that discriminated sound identity increased as the trial progressed (Figure 3D).

While both excitatory and inhibitory neurons showed stronger discrimination between sounds as trials progressed, a larger fraction of the inhibitory population were recruited toward the end of the task compared to the excitatory neuron population (Figure 3D, excitatory: dark blue, inhibitory: dark red, χ^2 test, $p < 0.01$). In contrast, during passive listening, these same PFC neurons failed to discriminate sound identity (Figure 3C), and the percentage of modulated neurons stayed low and constant throughout the auditory stimuli (Figure 3D). Together, these results demonstrate that PFC firing rates were modulated by auditory stimuli in a context-dependent manner. While both excitatory and inhibitory neurons showed greater discrimination ability as trials progressed, inhibitory neurons tended to be significantly more engaged towards trial completion.

PFC exhibits context- and outcome-dependent changes in LFP oscillation power

LFP oscillations have been broadly associated with many cognitive functions. To examine changes of LFP oscillations in the mouse PFC during the task, we analyzed LFP oscillations during both the “auditory discrimination” block and the “passive listening” block. We observed that LFP power was modulated at trial start and trial end during the discrimination task, but not during passive listening (Figures 4A1 and 4A2). More specifically, during the discrimination task, oscillation power first decreased across multiple

frequency bands upon trial initiation when compared to the powers before trial onset, then recovered in the middle of the trial, which subsequently decreased again at the trial end (Figures 4A1, before: blue, after: red, window size: 500 ms). Conversely, during passive listening, LFP powers remained constant (Figure 4A2, before: blue, after: red, window size: 500 ms).

To further examine the changes in power across mice, we calculated the z-score of LFP powers for each trial (2 second window centered at either trial start or trial end), and averaged across all trials for each animal. We then calculated the power for five frequency bands for each animal, alpha (5-8 Hz), theta (9-14 Hz), beta (15-30 Hz), low-gamma (30-50 Hz), and high-gamma (70-100 Hz), and averaged across all animals. Upon trial initiation, oscillation powers transiently decreased across all frequency bands from alpha to high-gamma (Figure 4C and E). Interestingly, for beta and low-gamma frequencies, we observed a brief rise in power before trial-start, which was not present in theta, alpha, or high-gamma frequencies. After the initial decrease, oscillation powers increased in the middle of the trial, and then decreased again towards the end of the trial at all frequencies (Figure 4D and F). In contrast, during the passive listening block, oscillation power largely stayed constant throughout the trial and progressed into the ITI. Closer examination revealed a small but significant increase across all frequencies upon cue presentation (Figure 4C and E), which is in sharp contrast to the observed decrease in oscillation powers during the discrimination task. At the end of the cue presentation period during passive listening, oscillation power decreased upon the termination of the auditory cue (Figure 4D and F). Together, these results demonstrate that PFC oscillatory activity is context and task progression dependent. The same auditory cues can result in broad reduction in oscillation powers during sensory discrimination, or slight increase during passive listening. Such observations highlight the correlation of dynamic changes in PFC oscillation patterns during the sensory discrimination task described here, consistent with that generally observed in other studies in other animal models.

We then examined whether LFP oscillations were differently modulated by task outcome. LFP oscillation power was modulated strongly when aligned to trial start, for both correct and incorrect trials (Figure 5 A1). However, when aligned to trial end, correct trials showed more dynamics than incorrect trials (Figure 5 A2). We further examined the changes in various frequency bands across all mice. At the start of a trial, oscillation powers decreased across all frequencies compared to that before trial-start during both the correct and the incorrect trials (Figure 5B). The fact that oscillations at higher frequencies (beta and gamma) were more suppressed in correct trials highlight the relevance of beta and gamma oscillations in mediating PFC related behaviors. The suppression of LFP powers, along with the selective increase in many individual PFC neurons' firing rate, suggests that changes in LFPs are mainly due to the synaptic inputs to the PFC, rather than PFC spiking alone.

To capture the difference in the oscillation dynamics between correct and incorrect trials, we calculated the average power for 500ms before versus after trial-start, and found that the drop in LFP power was larger in correct trials than in incorrect trials, except at alpha frequency (Figure 5D, N=5 mice, paired t-test, *: $p < 0.05$). When aligned to trial-end, oscillation powers diverged between the correct and the incorrect trials (Figure 5C). For correct trials, oscillation powers continued to decrease and remained low over a prolonged period into the ITI, across all frequencies (Figure 5C, black line). For incorrect trials, oscillation powers first decreased for a couple hundred milliseconds and then rose across all frequency bands (Figure 5C, gray line). As a result, the power changes at the trial end were significantly different between the correct and the incorrect trials (Figure 5D, N=5 mice, paired t-test, *: $p < 0.05$). The divergence of LFP powers at trial-end between correct and incorrect trials within a couple hundred milliseconds is interesting. However, we cannot rule out the possibility that this change reflects a difference in animal behavior, since in correct trials, animals retrieved a water reward, whereas in incorrect trials, animals experienced a 5-second timeout. Together, these results demonstrate that LFP

powers were in general decreased when animals started the task regardless of trial outcome, but the changes were great at trial-start during correct trials.

Inhibitory neurons exhibit higher spike-field coherence than excitatory neurons during distinct phases of auditory discrimination

To investigate the relationship between PFC spiking patterns and LFPs, we calculated spike-field coherence (SFC) between individual neurons and the LFPs recorded from the adjacent electrode within the ipsilateral hemisphere. We first examined whether the SFCs were selectively modulated by contexts. Among the 552 recorded neurons, 422 were from the recording sessions containing both discrimination blocks and the passive listening blocks. When aligned to trial start, SFCs at theta frequencies during the discrimination task exhibited a transient increase only at the beginning of the trial when compared to those during passive listening, which returned to approximately the same level in the middle of the trial (Figure 6A, left). SFCs then increased again toward trial end (Figure 6A, right). After the end of the trial, SFC showed no difference between the discrimination blocks and the passive listening blocks. Similar trends were observed for SFCs at alpha frequencies (Figure 6B). Interestingly, for beta frequencies, we observed a lower SFC during discrimination, but only in the middle of the trial (Figure 8C). For both low and high gamma frequencies, SFCs were lower during discrimination compared to passive listening at the trial start, which then reversed towards the trial end (Figure 6D and E).

Given that the pattern of LFP power changes across multiple frequencies was similar at trial-start (Figure 4A), the change in SFC at theta frequencies reflect stronger coupling of PFC spiking and theta oscillations, likely coordinated by inputs to the PFC. As trials progressed, SFCs became weaker at higher gamma frequencies, but stronger at lower theta to beta frequencies, and then at the end of the trial, SFCs rose across all frequencies except beta. Together, these results demonstrate wide spread changes

in SFC across all frequencies from alpha to high gamma. Similar to spike activity, the modulation of SFC was also context-dependent, which further suggest the difference in network states when animals were performing the task. Our results in general are in agreement with the idea that theta oscillations provide long-range connections between different brain regions, and gamma oscillations predominately parallel local spiking activities.

Although many studies have demonstrated that spikes and LFP oscillations are related to behavior, the details about how excitatory versus inhibitory neurons interact with oscillations are largely unknown. We compared SFCs between excitatory and inhibitory neurons. At trial start, inhibitory neurons exhibited higher coherence with higher frequency oscillations (both low- and high-gamma) (Figure 7D and E) than excitatory neurons, but not at lower frequencies (theta, alpha, and beta) (Figure 7A-C). As trials progressed, SFCs increased in both neuron types, but inhibitory neurons showed increasingly stronger coherence at lower frequencies (theta and alpha) that sustained beyond trial completion (Figure 7A and B). At higher frequencies (beta and low-gamma), the divergence of SFC between excitatory and inhibitory neurons only occurred after the trial end, where inhibitory neurons showed stronger coherence across almost all frequencies than excitatory neurons (Figure 7C and D). Interestingly, excitatory neurons showed higher coherence only at high gamma frequency bands, and only right before the end of the trial (Figure 7E). In summary, these results demonstrate that inhibitory neurons showed a stronger coherence with LFPs than excitatory neurons, across multiple frequencies, towards the end of the task. In contrast excitatory neurons only exhibit stronger coherence with the higher frequency gamma oscillations at trial-end. These results provide support for the idea that inhibitory neurons are critical in supporting higher beta and gamma frequency oscillations, whereas, lower frequency theta oscillations may provide long range coordination between the PFC and other areas.

Discussion

To understand the functional significance of excitatory versus inhibitory neurons and their relationships with LFP oscillation patterns in sensory discrimination in mice PFC, we performed tetrode recordings in mice performing a 3-choice auditory discrimination task. Using tetrodes, we distinguished excitatory neurons and inhibitory neurons based on spike waveforms, and found that inhibitory neurons were preferentially recruited at later stages, whereas excitatory neurons were most active at early stages of the trial. Inhibitory neurons also showed stronger spike-field coherence than excitatory neurons with LFP oscillations at high frequencies at task start, which switched to lower frequencies for the remaining period of the task. While oscillation power increased before both the start and the end of the task, the coherences between spiking activity and oscillations only rose at the end of the trial. Together, our results demonstrate that excitatory neurons and inhibitory neurons were recruited in a context-dependent manner at different phases of the task in mouse PFC, similar to the characteristic activity patterns in other species. The fact that inhibitory neurons exhibited a higher degree of coherence across all frequency bands is suggestive of inhibitory neural networks in supporting PFC oscillation dynamics, which may play a crucial role in organizing cell assemblies within the PFC in a context-dependent manner.

PFC neurons exhibit diverse response profiles during cognitive tasks, from task progression (Ma et al., 2014), to different aspects or stages of a task (Asaad et al., 1998). PFC neurons increase their firing rates when anticipating task-relevant sensory stimulation (Rodgers and DeWeese, 2014), responding to sensory stimuli presentation (Ninokura et al., 2004, Russ et al., 2008a), maintaining working memory (Rainer et al., 1998, Romo et al., 1999, Constantinidis et al., 2001, Kopec et al., 2015), predicting and/or anticipating reward (Matsumoto et al., 2003, Toda et al., 2012), or outcome (Amiez et al., 2006, Russ et al., 2008b, Hayden et al., 2011, Del Arco et al., 2017), which can linger into the inter-trial interval

(Marcos et al., 2016). We here show that mouse PFC neurons exhibit transient increases at specific stages of the task during a 3-choice discrimination task, suggesting that different subgroups of PFC neurons are recruited to process task-relevant information sequentially during our task.

PFC neurons have been shown to respond to task relevant auditory cues in many studies with a 2-choice auditory discrimination task. In this study, using a 3-choice auditory discrimination task allows us to examine more complex features of the PFC encoding ability. We found that, while a number of neurons increased their firing rate to only one auditory cue, many responded to two sounds. To a certain extent, these results suggest that PFC neurons can negatively respond to auditory cues of a certain identity. The combination of both positive and negative responses could expand the PFC's coding capacity; while an individual neuron could respond to multiple stimuli, ensemble of neurons could collectively represent or code a specific stimulus. It is interesting to speculate how such complex identification coding arises in the PFC, and how such coding scheme contributes to the discrimination process. Further experiments are needed to examine the detailed network mechanisms.

Different types of PFC neurons have been shown to exhibit distinct task-related responses (Hussar and Pasternak, 2009, 2012, Murray et al., 2015). Excitatory neurons increase their firing rates with less variability upon sensory stimulation (Hussar and Pasternak, 2010), whereas inhibitory neurons are more correlated with the later stage of a task, such as reward (Kvitsiani et al., 2013). Most recently, using optogenetics, Sparta et al. demonstrated that selective activation of PV neurons facilitated the extinction of cue-reward association (Sparta et al., 2014). We found that an increasing proportion of neurons, both excitatory and inhibitory, were modulated by auditory cues as the task progressed, suggesting gradual recruitment of the PFC neurons during sensory discrimination, consistent with the idea that the PFC accumulates information about sensory identity and outcome decision (Freedman et al., 2001). It is interesting that a higher fraction of inhibitory neurons was recruited towards the end of

the task. It is possible that inhibitory neurons were likely involved in associating task information with task outcome.

Although mice were presented with the same auditory cues in both the “discrimination task” and “passive-listening” blocks, the PFC was only modulated during the “discrimination task” block, indicating that PFC neurons’ activities are context-dependent. Such context-dependent modulation has been shown when animals were exposed to different environments (Hyman et al., 2012), or were performing tasks requiring different rules (White and Wise, 1999, Wallis et al., 2001, Stokes et al., 2013, Ma et al., 2016, Siniscalchi et al., 2016). In our study, almost all modulated neurons lost their modulation during the “passive-listening” blocks, suggesting a state difference when the animals were actively engaged in the task utilizing sensory information versus when they were passively presented with sensory information. Such state difference may involve many neuromodulators, such as acetylcholine and dopamine that have been shown to mediate attentional states (Del Arco et al., 2017).

Over the years, LFP oscillations at specific frequencies have been related to different aspects of behavioral tasks and states (Helfrich and Knight, 2016, Wimmer et al., 2016, Kamigaki and Dan, 2017), and LFP synchrony within the PFC and between the PFC and other areas has been observed in many tasks (Antzoulatos and Miller, 2016). In addition to single neuron responses in the PFC, we also observed wide spread changes in LFP oscillation patterns across all frequencies from alpha to high gamma, in general agreement with other studies. While beta oscillations have been associated with status quo and movement, in our current task, we cannot dissociate movement and task outcome. Interestingly, we observed that the power of oscillations reacted differently in response to task outcomes. We found that beta power first increased before trial onset, and then decreased upon sensory stimulation followed with a rebound, similar to previous reports where no movement was involved (Panagiotaropoulos et al., 2013). The oscillation power showed much stronger dynamics in correct trials than in incorrect trials, indicating the enhancement of oscillations may be crucial in successfully performing the task.

Spike-phase coherence at theta frequencies within the PFC and between the PFC and sensory areas increases during the delay period of working memory tasks (Liebe et al., 2012), whereas spike-field coherence at beta frequencies rose in monkey PFCs when monkeys were performing visual attention tasks (Buschman et al., 2012), and between PFCs and parietal cortex when monkeys performing category tasks (Antzoulatos and Miller, 2016). Moreover, phase-locking of pyramidal neurons to gamma oscillations in the PFC occurs during attentional processes (Kim et al., 2016b) and spiking activity is modulated by the phase of gamma oscillations in the visual cortex (Ni et al., 2016). Inhibitory neurons have been implicated in supporting LFP oscillations in the PFC (Lodge et al., 2009, Kim et al., 2016b) and other brain areas (Cardin et al., 2009, Miller et al., 2015). In our study, although the oscillation powers increased prior to both trial-initiation and trial completion, only the latter is associated with an increase in spike-field coherence, suggesting that the same oscillation frequencies may serve different functions depending on the ongoing task. More interestingly, while changes in oscillations patterns are similar across multiple frequency bands during the task, their interactions with spikes differ depending on the LFP frequency bands and cell types. In general, inhibitory neurons showed stronger coherence than excitatory neurons in a trial progression-dependent manner. These results further support the rationale that inhibitory neurons play an important role in generating or supporting beta and gamma frequency oscillations.

Materials and methods

Three--choice auditory discrimination task

Behavior Arena

The behavior arena (12 inch x 12 inch) was constructed with black plastic walls and a mesh floor. The start location was located at one side of the arena (1 inch away from the wall), and three reward

locations were at the opposite side (1 inch away from the wall) (Figure 1). Each location was equipped with an IR beam sensor and a white LED light on the floor. A speaker was located outside of the box, at the reward side, and delivered a 70 db auditory cue when the animal initiated the task. The room had a consistent background noise of approximately 60 db. LabVIEW (2012, National Instruments, Austin, TX) scripts were used to control the sensors and LED lights in the behavior arena via a NiDAQ board (NI USB-6259, National Instruments, Austin, TX) and recorded behavior events.

Behavioral training

All animal procedures were approved by the Boston University Institutional Animal Care and Use Committee. Female C57BL/6 mice (Taconic, Hudson, NY), were water-restricted during behavioral testing, and were closely monitored to ensure that they maintained at least 85% of their pre-experiment body weight. Adult female mice (2-3 months old at the start of the experiments) were trained to perform a 3-choice auditory discrimination task in following steps:

Step 1: Obtain water from reward port. At this step, only the middle reward port was accessible to the animal. It delivered a water reward whenever an animal reached the reward location and triggered the IR beam sensor in front of the water port.

Step 2: Detection of the first auditory cue. A white LED at the start location was illuminated to indicate trial initiation. Mice learned through trial and error to initiate a trial by reaching the start location, which triggered the IR beam sensor and the first auditory cue was presented. Mice were allowed to reach the reward location to obtain the reward without any time limit.

Step 3: Detection of the second auditory cue. After the animal learned initiating the task and responding to the first cue, we made the reward location associated with the second cue accessible, while blocking the reward locations for the other two cues. At this step, when animals initiated a trial, only the second

cue was presented, and animals were required to reach the corresponding location for reward with no time limit.

Step 4: Two-choice auditory discrimination task. At this step, the reward locations for both the first and the second cues were accessible. When animals initiated the trial, one of two auditory cues would be presented randomly, and mice were required to reach the corresponding reward location for reward with no time limit. When animals reached the incorrect reward location, a 5 second timeout occurred, indicated by white LED lights around the reward locations.

Step 5: Detection of the third auditory cue: After the animal learned the 2-choice discrimination task, we repeated Step 3 to introduce the third auditory cue. At this step, only the third reward location was accessible and the other two were blocked. When an animal initiated the trial, only the third auditory cue was played, and the animal was required to reach the third reward location to complete the trial and receive the reward with no time limit.

Step 6: Three-choice auditory discrimination task. All three reward ports were accessible. When animals initiated the trial, one of the three auditory cues was presented, and mice were required to reach the corresponding reward location to obtain reward. At this stage, a reaction time limit of 5 seconds was introduced. Failure of reaching the reward location within 5 seconds would cause a timeout, indicated by white LED lights around the reward locations. To obtain a balanced number of trials with each cue, auditory cues were presented in a group of three, and within each group, each auditory cue was presented once in a random order.

During training, each mouse was trained 20 minutes per day. Once well trained, defined as performing over 60% correct rate per day over 3 consecutive training days and capable of completing a minimum of 100 trials per day, animals were provided free water access in their home cage for a week and then underwent tetrode implantation. After tetrode implantation and recovery from surgery, animals were

briefly re-trained using procedures described in Steps 2-6 until their performance reached 60%, and then recordings were performed.

Electrophysiology

Custom tetrode devices (16 channels) were assembled in house, which contained four tetrode bundles, two bundles targeting each hemisphere. The four tetrode bundles were designed to target the PFC bilaterally (AP: +1.8, ML: +0.2; AP: +2.2; ML +0.2; AP: 2.2; ML: -0.2; AP 2.2, ML: +0.2). A tetrode bundle was made by twisting together 4 tetrode wires (Sandvik-Kanthal, Ahmerst, NY), and adjusting the impedance to 0.5-1 MOhm with gold plating (SIFCO 5355, SIFCO ASC, Independence, Ohio). Tetrodes were implanted with the center positioned at the midline (AP: 2, ML: 0), so that the tetrode bundles targeted the PFC (AP: 2+/-0.2, ML: +/- 0.2). We advanced tetrode bundles gradually during the re-training period, so that the tip of the tetrode bundles reached the PFC at the recording stage (AP: 1.0 – 1.9). All recordings were performed in freely-moving mice. During recording, the tetrode device was connected to a commutator (ACO32, Tucker-Davis Technologies, Alachua, FL) to ensure free movement in the behavior arena. Data was acquired with a Plexon OmniPlex system (Plexon Inc, Dallas, TX). Spike waveforms and local field potentials were sampled at 40 kHz and at 1 kHz respectively. The Plexon OmniPlex system also received time stamps from the NiDAQ board to record timing of behavioral events.

Mice underwent one recording session per day. Each recording session constituted one “discrimination task” block and one “passive listening” block in random order. Animals could move freely in the behavioral arena during the entire recording session. The “discrimination task” block lasted about 20 minutes, and animals were allowed to initiate the task as many times as they desired. In general, mice performed 100-200 trials within 20 minutes. During the “passive listening” block, mice were placed in the same behavioral arena with a plastic floor positioned above all IR beam sensors and LEDs, so that

mice had no access to any sensors or water ports. The same three auditory cues (~70db) used in the “discrimination task” were played in pseudo-random order for 200-250 trials. The durations of the auditory cues were randomized from 1.5 to 3 seconds with random 1.5 - 3 seconds inter-trial intervals.

Data analysis

Spike: Spikes were sorted with Offline Sorter (Plexon Inc, Dallas, TX) and then imported into Matlab (2014, MathWorks, Natick, MA) for further analysis. Spike width was defined as the duration between the valley and the peak of a spike waveform. Due to the difference in lengths of each trial, to calculate the firing rate throughout trial progression, we first normalized each trial based on its duration, so that trial start and trial end were aligned at 0% and at 100% of trial progression, respectively. We then calculated the firing rate from -20% to +120% of trial progression using a 1% moving window, and smoothed the results by averaging each data point with its two adjacent data points. When presenting the population data, we further normalized the firing rate between -20% to 120% of trial progression by calculating the z-scores for each neuron with its own mean and standard deviation.

LFP: LFPs were imported into Matlab with the Matlab custom script provided by Plexon, and then analyzed with the Chronux toolbox (chronux.org). The power spectrogram of each LFP trace was calculated with mtspecgramc function (moving window size: 500 ms, moving window step: 5ms, tapers: [3 5]) in Chronux.

In a few occasions, animal movement caused artifacts in our tetrode recording, such as when the tetrode devices bumped the arena walls, which create large voltage deflections in our recordings. To eliminate the impact of such movement artifact in our analysis, we identified these artifact periods as having the 5% maximum amplitude, either positive or negative, of the whole recording session. Trials that contained these artifact periods were excluded from all analysis involving LFPs.

The spectrogram examples shown in Fig. 5A were log-normalized ($10 \cdot \log(\text{power}/\text{max})$), with the maximum power of either the whole recording session (Figure 5A), or of the examined time window (2 second, centered at either trial start or end) (Figures 5B and 7A, averaged across trials). To compare the powers at specific frequency bands across mice, the powers within the examined time window (2 second, centered at either trial start or end) of each trial were first normalized by converting to their z-scores and then averaged within a given frequency band to obtain the power of each trial. The powers of all trials from the same animal were then averaged as the power of each animal. In our analysis, we examined five frequency bands, and the ranges of each frequency bands were defined as follows: alpha (5-8 Hz), theta (9-14 Hz), beta (15-30 Hz), low-gamma (30-50 Hz), and high-gamma (70-100 Hz).

Spike-field coherence was calculated with cohgramcpt function (moving window size: 500 ms, moving window step: 5ms, tapers: [3 5]) in Chronux. For each trial, we first calculated the spike-field coherence for each neuron with LFPs at a specific frequency range, and then averaged across trials.

Statistical testing

For spike rate modulation, we used one-way ANOVA to compare the firing rates at the same trial progression period for different auditory cues. For LFP power spectrum, we used a paired t-test to compare the power during the 500 ms before and after either trial start or trial end. For spike-field coherence, we used a non-paired t-test to compare the coherence at the same trial progression period between the “discrimination task” blocks and “passive listening” blocks. All analyses were performed in Matlab. Details for each test are presented throughout the Results section.

Data Availability

The datasets generated during and/or analysed during the current study are available from the corresponding author on reasonable request.

References

- Amiez C, Joseph JP, Procyk E (2006) Reward encoding in the monkey anterior cingulate cortex. *Cerebral cortex* 16:1040-1055.
- Antzoulatos EG, Miller EK (2016) Synchronous beta rhythms of frontoparietal networks support only behaviorally relevant representations. *Elife* 5.
- Asaad WF, Rainer G, Miller EK (1998) Neural activity in the primate prefrontal cortex during associative learning. *Neuron* 21:1399-1407.
- Buschman TJ, Denovellis EL, Diogo C, Bullock D, Miller EK (2012) Synchronous oscillatory neural ensembles for rules in the prefrontal cortex. *Neuron* 76:838-846.
- Cardin JA, Carlen M, Meletis K, Knoblich U, Zhang F, Deisseroth K, Tsai LH, Moore CI (2009) Driving fast-spiking cells induces gamma rhythm and controls sensory responses. *Nature* 459:663-667.
- Cardin JA, Palmer LA, Contreras D (2007) Stimulus feature selectivity in excitatory and inhibitory neurons in primary visual cortex. *The Journal of neuroscience : the official journal of the Society for Neuroscience* 27:10333-10344.
- Cho KK, Hoch R, Lee AT, Patel T, Rubenstein JL, Sohal VS (2015) Gamma rhythms link prefrontal interneuron dysfunction with cognitive inflexibility in *Dlx5/6*(+/-) mice. *Neuron* 85:1332-1343.
- Constantinidis C, Franowicz MN, Goldman-Rakic PS (2001) The sensory nature of mnemonic representation in the primate prefrontal cortex. *Nature neuroscience* 4:311-316.
- Dalley JW, Cardinal RN, Robbins TW (2004) Prefrontal executive and cognitive functions in rodents: neural and neurochemical substrates. *Neurosci Biobehav Rev* 28:771-784.

503 Dejean C, Courtin J, Karalis N, Chaudun F, Wurtz H, Bienvenu TC, Herry C (2016) Prefrontal neuronal
504 assemblies temporally control fear behaviour. *Nature* 535:420-424.

505 Del Arco A, Park J, Wood J, Kim Y, Moghaddam B (2017) Adaptive encoding of outcome prediction by
506 prefrontal cortex ensembles supports behavioral flexibility. *J Neurosci*.

507 Duan CA, Erlich JC, Brody CD (2015) Requirement of Prefrontal and Midbrain Regions for Rapid Executive
508 Control of Behavior in the Rat. *Neuron* 86:1491-1503.

509 Freedman DJ, Riesenhuber M, Poggio T, Miller EK (2001) Categorical representation of visual stimuli in
510 the primate prefrontal cortex. *Science* 291:312-316.

511 Gibson JR, Beierlein M, Connors BW (1999) Two networks of electrically coupled inhibitory neurons in
512 neocortex. *Nature* 402:75-79.

513 Gregoriou GG, Gotts SJ, Zhou H, Desimone R (2009) High-frequency, long-range coupling between
514 prefrontal and visual cortex during attention. *Science* 324:1207-1210.

515 Gregoriou GG, Rossi AF, Ungerleider LG, Desimone R (2014) Lesions of prefrontal cortex reduce
516 attentional modulation of neuronal responses and synchrony in V4. *Nat Neurosci* 17:1003-1011.

517 Han X, Qian X, Bernstein JG, Zhou HH, Franzesi GT, Stern P, Bronson RT, Graybiel AM, Desimone R,
518 Boyden ES (2009) Millisecond-timescale optical control of neural dynamics in the nonhuman
519 primate brain. *Neuron* 62:191-198.

520 Hanks TD, Summerfield C (2017) Perceptual Decision Making in Rodents, Monkeys, and Humans. *Neuron*
521 93:15-31.

522 Hayden BY, Pearson JM, Platt ML (2011) Neuronal basis of sequential foraging decisions in a patchy
523 environment. *Nature neuroscience* 14:933-939.

524 Helfrich RF, Knight RT (2016) Oscillatory Dynamics of Prefrontal Cognitive Control. *Trends in cognitive*
525 *sciences*.

526 Hussar C, Pasternak T (2010) Trial-to-trial variability of the prefrontal neurons reveals the nature of their
527 engagement in a motion discrimination task. *Proceedings of the National Academy of Sciences*
528 of the United States of America 107:21842-21847.

529 Hussar CR, Pasternak T (2009) Flexibility of sensory representations in prefrontal cortex depends on cell
530 type. *Neuron* 64:730-743.

531 Hussar CR, Pasternak T (2012) Memory-guided sensory comparisons in the prefrontal cortex:
532 contribution of putative pyramidal cells and interneurons. *The Journal of neuroscience : the*
533 official journal of the Society for Neuroscience 32:2747-2761.

534 Hyman JM, Ma L, Balaguer-Ballester E, Durstewitz D, Seamans JK (2012) Contextual encoding by
535 ensembles of medial prefrontal cortex neurons. *Proceedings of the National Academy of*
536 *Sciences of the United States of America* 109:5086-5091.

537 Kamigaki T, Dan Y (2017) Delay activity of specific prefrontal interneuron subtypes modulates memory-
538 guided behavior. *Nat Neurosci* 20:854-863.

539 Kim D, Jeong H, Lee J, Ghim JW, Her ES, Lee SH, Jung MW (2016a) Distinct Roles of Parvalbumin- and
540 Somatostatin-Expressing Interneurons in Working Memory. *Neuron*.

541 Kim H, Ahrlund-Richter S, Wang X, Deisseroth K, Carlen M (2016b) Prefrontal Parvalbumin Neurons in
542 Control of Attention. *Cell* 164:208-218.

543 Kopec CD, Erlich JC, Brunton BW, Deisseroth K, Brody CD (2015) Cortical and Subcortical Contributions to
544 Short-Term Memory for Orienting Movements. *Neuron* 88:367-377.

545 Kvitsiani D, Ranade S, Hangya B, Taniguchi H, Huang JZ, Kepecs A (2013) Distinct behavioural and
546 network correlates of two interneuron types in prefrontal cortex. *Nature* 498:363-366.

547 Lagler M, Ozdemir AT, Lagoun S, Malagon-Vina H, Borhegyi Z, Hauer R, Jelem A, Klausberger T (2016)
548 Divisions of Identified Parvalbumin-Expressing Basket Cells during Working Memory-Guided
549 Decision Making. *Neuron* 91:1390-1401.

550 Lee JH, Russ BE, Orr LE, Cohen YE (2009) Prefrontal activity predicts monkeys' decisions during an
551 auditory category task. *Front Integr Neurosci* 3:16.

552 Lee K, Holley SM, Shobe JL, Chong NC, Cepeda C, Levine MS, Masmanidis SC (2017) Parvalbumin
553 Interneurons Modulate Striatal Output and Enhance Performance during Associative Learning.
554 *Neuron* 93:1451-1463 e1454.

555 Liebe S, Hoerzer GM, Logothetis NK, Rainer G (2012) Theta coupling between V4 and prefrontal cortex
556 predicts visual short-term memory performance. *Nature neuroscience* 15:456-462, S451-452.

557 Lodge DJ, Behrens MM, Grace AA (2009) A loss of parvalbumin-containing interneurons is associated
558 with diminished oscillatory activity in an animal model of schizophrenia. *The Journal of*
559 *neuroscience : the official journal of the Society for Neuroscience* 29:2344-2354.

560 Lundqvist M, Rose J, Herman P, Brincat SL, Buschman TJ, Miller EK (2016) Gamma and Beta Bursts
561 Underlie Working Memory. *Neuron* 90:152-164.

562 Ma L, Hyman JM, Durstewitz D, Phillips AG, Seamans JK (2016) A Quantitative Analysis of Context-
563 Dependent Remapping of Medial Frontal Cortex Neurons and Ensembles. *J Neurosci* 36:8258-
564 8272.

565 Ma L, Hyman JM, Phillips AG, Seamans JK (2014) Tracking progress toward a goal in corticostriatal
566 ensembles. *The Journal of neuroscience : the official journal of the Society for Neuroscience*
567 34:2244-2253.

568 Marcos E, Tsujimoto S, Genovesio A (2016) Event- and time-dependent decline of outcome information
569 in the primate prefrontal cortex. *Scientific reports* 6:25622.

570 Matsumoto K, Suzuki W, Tanaka K (2003) Neuronal correlates of goal-based motor selection in the
571 prefrontal cortex. *Science* 301:229-232.

572 Miller CT, Thomas AW, Nummela SU, de la Mothe LA (2015) Responses of primate frontal cortex
573 neurons during natural vocal communication. *J Neurophysiol* 114:1158-1171.

574 Miller EK (2000) The prefrontal cortex and cognitive control. *Nature reviews Neuroscience* 1:59-65.

575 Miller EK, Cohen JD (2001) An integrative theory of prefrontal cortex function. *Annu Rev Neurosci*

576 24:167-202.

577 Mitchell JF, Sundberg KA, Reynolds JH (2007) Differential attention-dependent response modulation

578 across cell classes in macaque visual area V4. *Neuron* 55:131-141.

579 Murray AJ, Woloszynowska-Fraser MU, Ansel-Bollepalli L, Cole KL, Foggetti A, Crouch B, Riedel G, Wulff P

580 (2015) Parvalbumin-positive interneurons of the prefrontal cortex support working memory and

581 cognitive flexibility. *Scientific reports* 5:16778.

582 Ni J, Wunderle T, Lewis CM, Desimone R, Diester I, Fries P (2016) Gamma-Rhythmic Gain Modulation.

583 *Neuron* 92:240-251.

584 Ninokura Y, Mushiake H, Tanji J (2004) Integration of temporal order and object information in the

585 monkey lateral prefrontal cortex. *Journal of neurophysiology* 91:555-560.

586 Panagiotaropoulos TI, Kapoor V, Logothetis NK (2013) Desynchronization and rebound of beta

587 oscillations during conscious and unconscious local neuronal processing in the macaque lateral

588 prefrontal cortex. *Frontiers in psychology* 4:603.

589 Pinto L, Dan Y (2015) Cell-Type-Specific Activity in Prefrontal Cortex during Goal-Directed Behavior.

590 *Neuron* 87:437-450.

591 Rainer G, Asaad WF, Miller EK (1998) Selective representation of relevant information by neurons in the

592 primate prefrontal cortex. *Nature* 393:577-579.

593 Rodgers CC, DeWeese MR (2014) Neural correlates of task switching in prefrontal cortex and primary

594 auditory cortex in a novel stimulus selection task for rodents. *Neuron* 82:1157-1170.

595 Romanski LM, Goldman-Rakic PS (2002) An auditory domain in primate prefrontal cortex. *Nat Neurosci*

596 5:15-16.

597 Romo R, Brody CD, Hernandez A, Lemus L (1999) Neuronal correlates of parametric working memory in
598 the prefrontal cortex. *Nature* 399:470-473.

599 Rossi AF, Bichot NP, Desimone R, Ungerleider LG (2007) Top down attentional deficits in macaques with
600 lesions of lateral prefrontal cortex. *J Neurosci* 27:11306-11314.

601 Russ BE, Ackelson AL, Baker AE, Cohen YE (2008a) Coding of auditory-stimulus identity in the auditory
602 non-spatial processing stream. *J Neurophysiol* 99:87-95.

603 Russ BE, Orr LE, Cohen YE (2008b) Prefrontal neurons predict choices during an auditory same-different
604 task. *Curr Biol* 18:1483-1488.

605 Siniscalchi MJ, Phoumthipphavong V, Ali F, Lozano M, Kwan AC (2016) Fast and slow transitions in
606 frontal ensemble activity during flexible sensorimotor behavior. *Nature neuroscience*.

607 Sparta DR, Hovelso N, Mason AO, Kantak PA, Ung RL, Decot HK, Stuber GD (2014) Activation of
608 prefrontal cortical parvalbumin interneurons facilitates extinction of reward-seeking behavior.
609 *The Journal of neuroscience : the official journal of the Society for Neuroscience* 34:3699-3705.

610 Stokes MG, Kusunoki M, Sigala N, Nili H, Gaffan D, Duncan J (2013) Dynamic coding for cognitive control
611 in prefrontal cortex. *Neuron* 78:364-375.

612 Toda K, Sugase-Miyamoto Y, Mizuhiki T, Inaba K, Richmond BJ, Shidara M (2012) Differential encoding of
613 factors influencing predicted reward value in monkey rostral anterior cingulate cortex. *PloS one*
614 7:e30190.

615 Wallis JD, Anderson KC, Miller EK (2001) Single neurons in prefrontal cortex encode abstract rules.
616 *Nature* 411:953-956.

617 Watrous AJ, Fell J, Ekstrom AD, Axmacher N (2015) More than spikes: common oscillatory mechanisms
618 for content specific neural representations during perception and memory. *Curr Opin Neurobiol*
619 31:33-39.

White IM, Wise SP (1999) Rule-dependent neuronal activity in the prefrontal cortex. *Experimental brain research* 126:315-335.

Wimmer K, Ramon M, Pasternak T, Compte A (2016) Transitions between Multiband Oscillatory Patterns Characterize Memory-Guided Perceptual Decisions in Prefrontal Circuits. *The Journal of neuroscience : the official journal of the Society for Neuroscience* 36:489-505.

Womelsdorf T, Fries P, Mitra PP, Desimone R (2006) Gamma-band synchronization in visual cortex predicts speed of change detection. *Nature* 439:733-736.

Acknowledgements

We thank members of Han lab for suggestions on the manuscript.

Author Contributions

H.T and X.H. designed all experiments and wrote the paper. H.T. performed experiments and data analysis. X.H. supervised the project.

Financial Disclosure

X.H. acknowledges funding from NIH Director's Office (1DP2NS082126), NIMH (5R00MH085944), the Grainger Foundation, the Pew Foundation, Brain and Behavior Research Foundation, Boston University Biomedical Engineering Department.

Competing Interests

The author(s) declare no competing interests.

Figure Legends

Figure 1. Recording of excitatory and inhibitory neurons during a three-choice auditory discrimination

behavioral task. (A) During the auditory discrimination task, mice self-initiated each trial by triggering a motion detector at the “initiation” location. Upon trial-start, one of three auditory stimuli were presented throughout the trial. On the other end of the arena, there were three reward locations, each paired with a specific auditory stimulus. Mice were given 5 seconds to reach one of the three reward locations. If mice reached the correctly paired reward location, a reward was provided. If mice failed to reach the correct reward location, they experienced a 5 second timeout period, with a bright light illuminating the arena. (B) The behavioral performance of mice during the first three recording sessions (left) and the last three recording sessions (right). All mice had correct rates above random chance of 33% (N=6 mice). (C) The reaction time during the first three recording sessions (left) and last three recording sessions (right). Each line represents mean \pm std of an individual mouse. (D) Representative waveforms of excitatory (D1) and inhibitory (D2) neurons recorded with tetrode bundles. (E) Binomial distribution of the width of spike waveforms, with a clear separation at 0.4 milliseconds between the two peaks, which was used as a threshold to identify excitatory (blue) and inhibitory (red) neurons.

Figure 2. Context and stage-dependent modulation of spiking activity. (A, B and C) Raster plots from two representative excitatory neurons (A and B), and one inhibitory neuron (C) during the discrimination tasks (A1, B1, C1) and during passive listening (A2, B2, C2). Normalized firing rates throughout trial progression across all trials in the discrimination task (A3-C3, blue lines) and the passive listening condition (A3-C3, gray lines). PFC neurons showed elevated firing rates at trial-start (A), in the middle of the task (B), and at trial-end (C). (D) Normalized population firing rate during the discrimination task (D1)

and during passive listening (D2, sorted in the same order as in D1; 130 neurons tested only in discrimination block, but not in passive listening block are filled with dark blue). Neurons were grouped by type (excitatory and inhibitory) and sorted based on the timing of their peak firing rates. (E) Distribution of excitatory (blue bars) and inhibitory neurons (red bars) based on the timing of the peak firing rate.

Figure 3. Heterogeneous responses of PFC neurons to different auditory cues. (A) One representative neuron with increased response to the presentation of one auditory cue (25 click/sec), but not to the other two (10 kHz sine wave and 100 click/sec). *Left*: raster plot of spikes for trials with different auditory cues presentation (blue: 10 kHz sine wave; red: 25 click/sec; green: 100 click/sec), and sorted by trial durations. *Right*: normalized firing rate during each auditory stimulus across trials. (B) Another example neuron positively modulated by two auditory cues (10 kHz sine wave and 100 click/sec), but not a third (25 click/sec). (C) Modulations of each neuron presented as p-values calculated with one-way ANOVA over trial progression. Neurons were grouped as excitatory (top) and inhibitory neurons (bottom), and sorted by the total duration when they were modulated. Modulations only occurred during the discrimination task (C1), but not during the passive-listening condition (C2, the neurons are sorted in the same order as C1). (D) The percentage of modulated excitatory (blue) and inhibitory (red) neurons throughout trial progression. During the task, the percentage of modulated excitatory neurons (blue, dot line) and inhibitory neurons (red, solid line) increased as the trial progressed; during passive listening, however, the percentage of modulated neurons remained constant (excitatory: blue, dot line. inhibitory: red, dot line).

Figure 4. Changes in LFP oscillation powers during auditory discrimination versus passive listening. (A) An example of LFP oscillation during the discrimination task (A1) and during passive listening (A2) from the same recording session. Average spectrograms (top) aligned at trial-start (left) and trial-end (right). (B) Average LFP powers during discrimination task (B1) and during passive listening (B2) at trial-start

(left, blue and red: 500 ms window before and after trial start, respectively) and at trial-end (right, blue and red: 500 ms window before and after trial start, respectively). (C and D) Normalized population LFP oscillation powers across animals (N=5) at theta (5-8 Hz), alpha (8-14 Hz), beta (15-30 Hz), low-gamma (40-50 Hz), and high-gamma frequencies (70-100 Hz), aligned at trial-start (C, discrimination task: black, passive listening: gray) or at trial-end (D, discrimination task: black, passive listening: gray). LFP powers were normalized as z-scores to the 2 second window centered at either trial-start (C) or trial-end (D). Shaded areas indicate standard error. (E and F) During discrimination task, decrease in LFP powers across all frequency bands after trial initiation (E1, N=5, paired t-test, *: $p < 0.05$) and again when the animal completed the trial (F1, N=5, paired t-test, *: $p < 0.05$). During the passive listening condition, LFP powers in all frequency bands increased at trial-start (E2; N=5, paired t-test, *: $p < 0.05$) and decreased at trial-end (F2; N=5, paired t-test, *: $p < 0.05$). Error bars indicate standard deviation.

Figure 5. LFP oscillation power diverged between correct and incorrect trials at the end of the trial.

(A) Spectrogram of the correct trials (A1) and the incorrect trials (A2) from one representative recording session, aligned to trial-start (left) and to trial-end (right). (B) Normalized population LFP oscillation powers of correct (black line) and incorrect (gray line) trials, aligned to trial-start. LFP powers at all frequency bands decreased after the animals initiated the trial; however, the differences in power were larger in correct trials than in incorrect trials (D1, N=5, paired t-test, *: $p < 0.05$). (C) Normalized population power of correct (black line) and incorrect (gray line) trials at trial end. LFP power of correct trials exhibited a prolonged suppression, while those of incorrect trials recovered and further increased (D2, N=5 mice, paired t-test, *: $p < 0.05$).

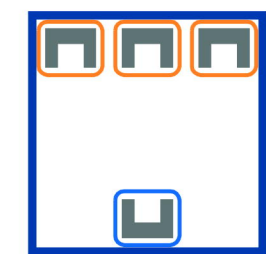
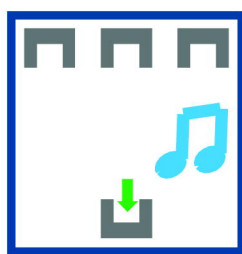
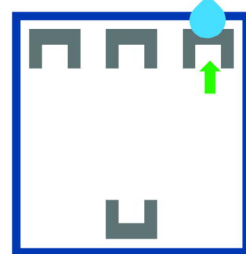
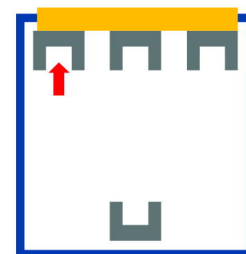
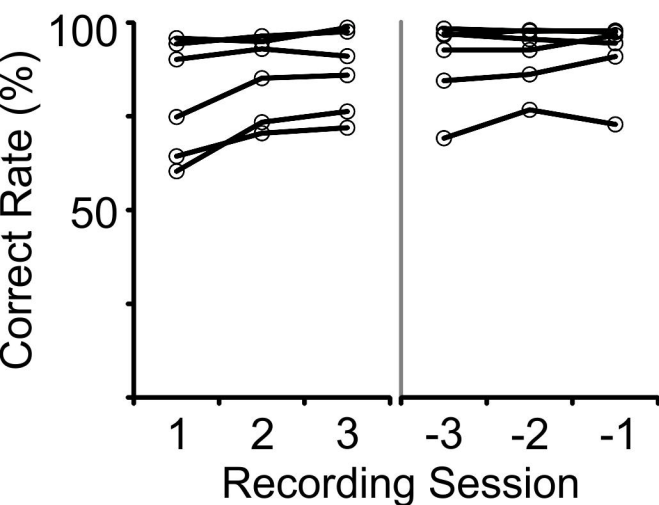
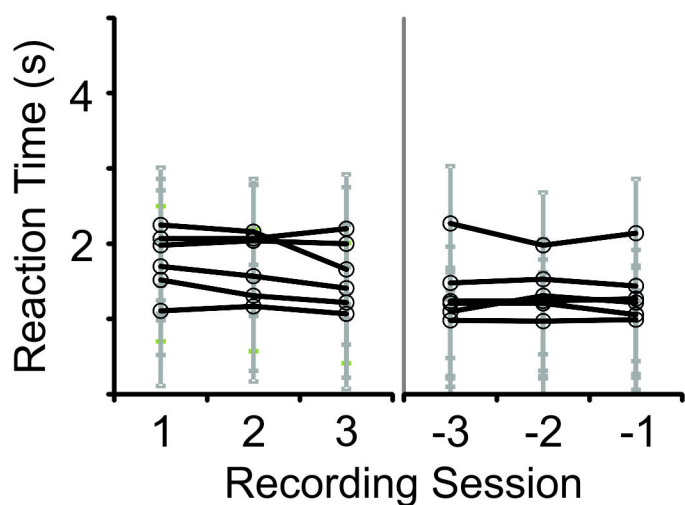
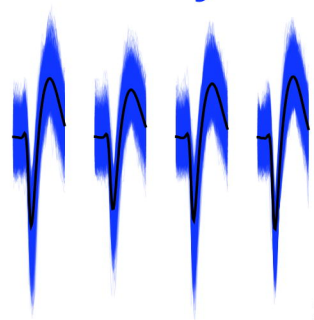
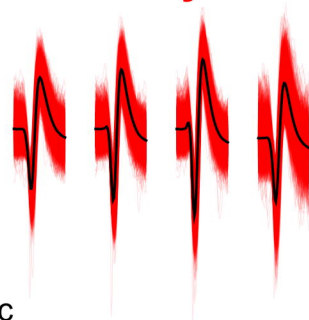
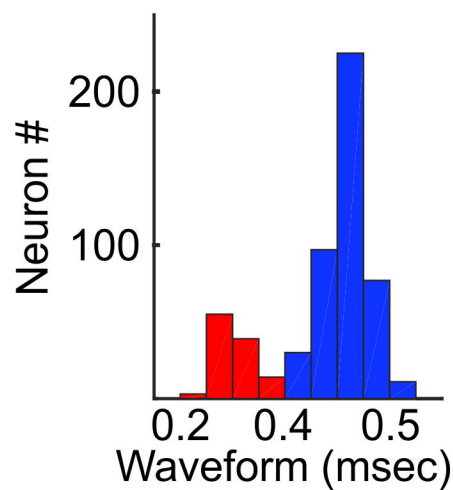
Figure 6. Spike-field coherence during auditory discrimination versus during passive listening.

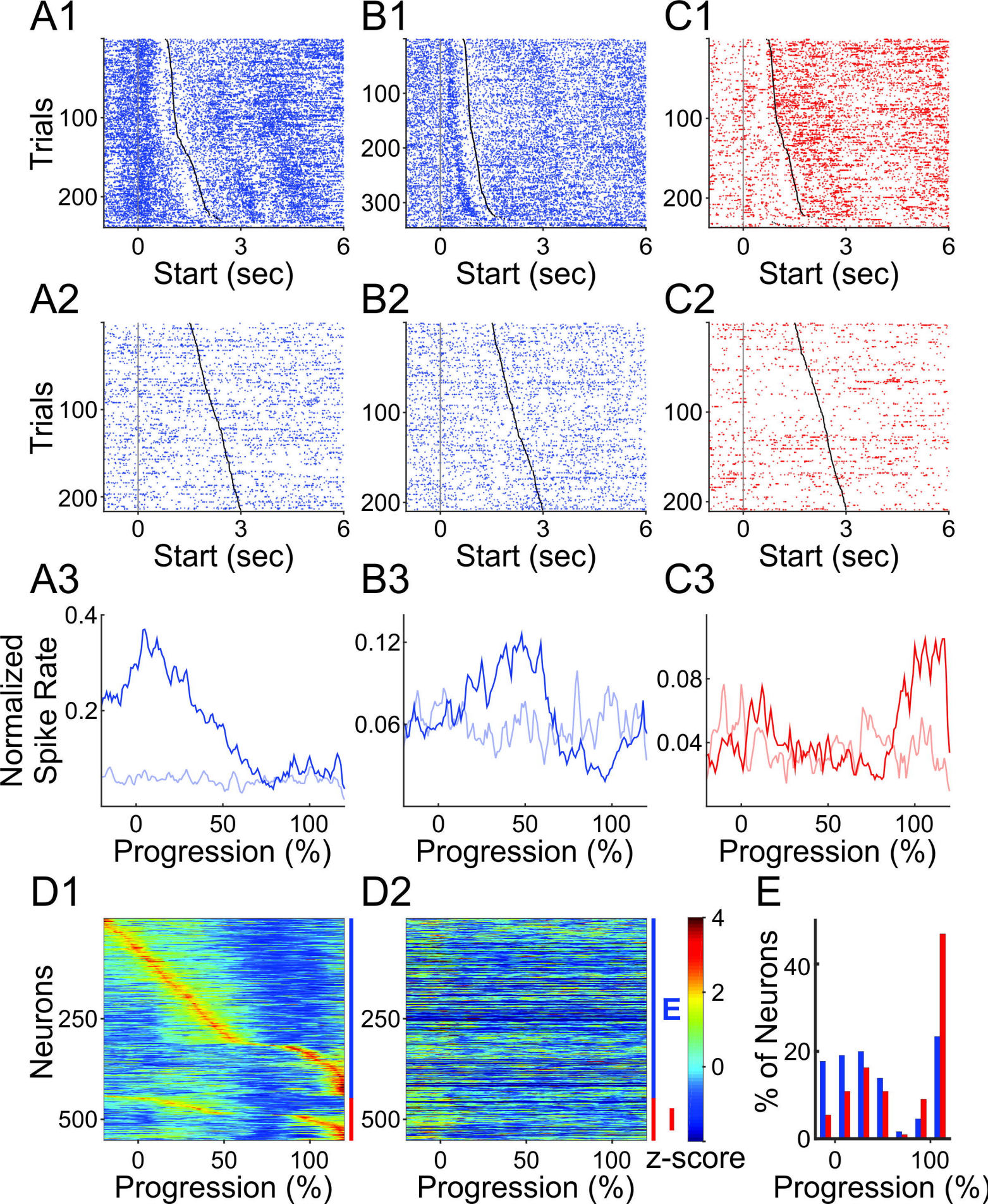
The spike-field coherence (SFC) at trial-start (left) and trial-end (right) during the discrimination task (black line, mean \pm s.e.m) and passive listening (gray line, mean \pm s.e.m) at theta (A), alpha (B), beta (C), low gamma (D) and high gamma (E) frequencies. (N=422 neurons, t-test, *: $p < 0.05$).

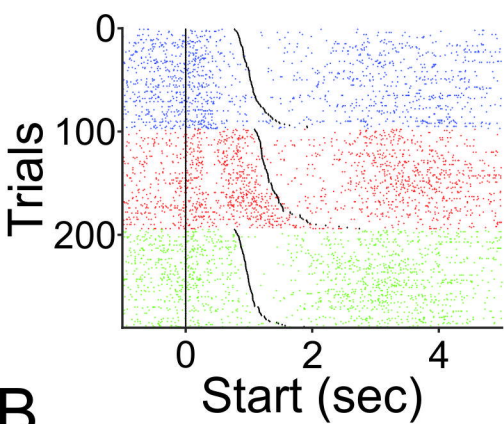
Figure 7. Inhibitory neurons exhibited stronger coherence with LFP than excitatory neurons. The spike-field coherences of excitatory neurons (blue, mean \pm s.e.m) and inhibitory neurons (red, mean \pm s.e.m) at trial-start (left) and trial-end (right) during the discrimination task. (A and B) At alpha (A) and theta (B) frequencies, there was no difference in SFCs between excitatory and inhibitory neurons at trial-start (left). Towards trial-end, inhibitory neurons showed higher SFCs than excitatory neurons, and the elevation sustained beyond trial-end (right). (C) At beta frequencies, inhibitory neurons transiently showed higher SFCs at trial-end. (D) At low-gamma frequencies, inhibitory neurons showed higher SFCs at trial-start (left) and trial-end (right), but not in the middle of the trial. (E) At high-gamma frequencies, inhibitory neurons showed higher SFCs at trial-start (left), while excitatory neurons showed higher SFCs in the middle of the trial (right). (Excitatory = 331 neurons, inhibitory= 91 neurons, t-test, *: $p < 0.05$).

Supplemental Figure Legends

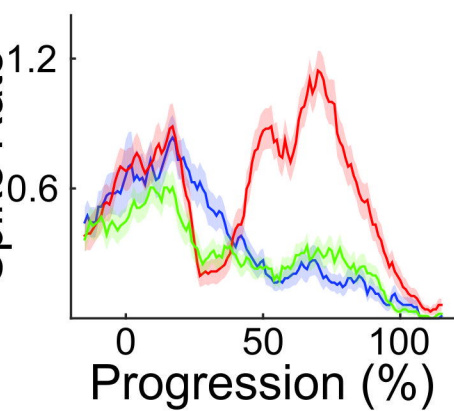
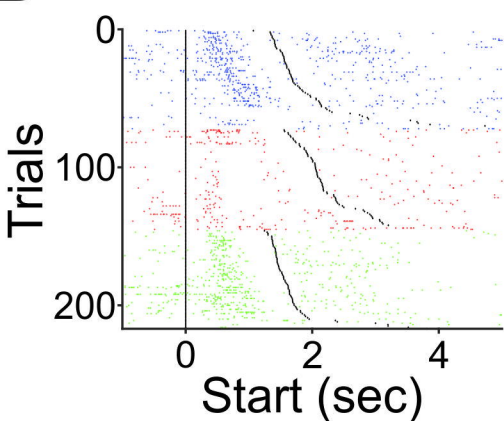
Figure S1. PFC spiking activity during correct versus incorrect trials. (Related to Figure 2) Normalized population firing rates of excitatory (blue) and inhibitory (red) neurons during correct trials (A), and incorrect trials (B).

A**Behavior Arena****Reward Locations****Initiation Location****Behavior Paradigm****Self-Initiation****Correct: Reward****Incorrect: Timeout****B****C****D1****Excitatory****D2****Inhibitory****E**

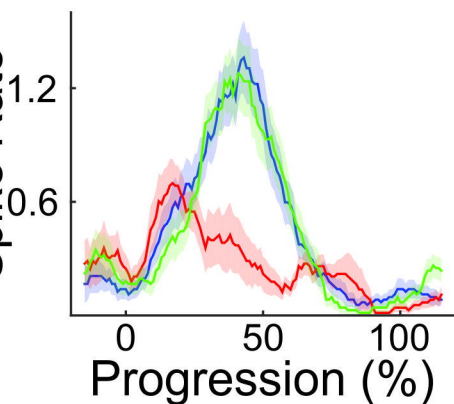
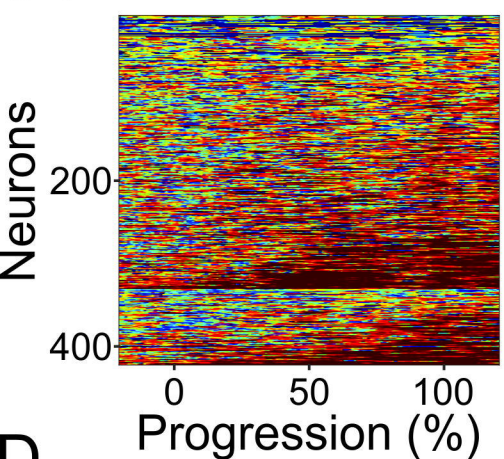
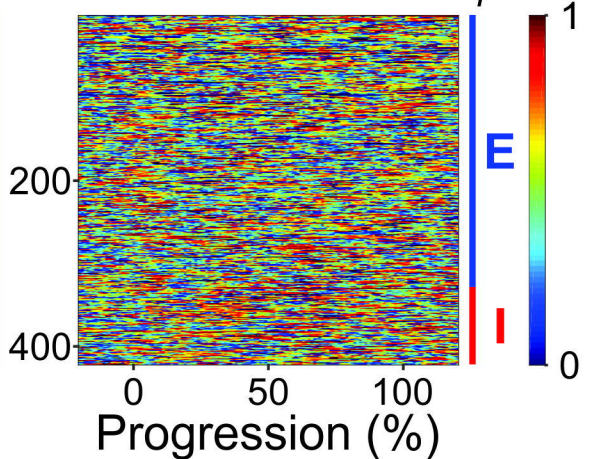
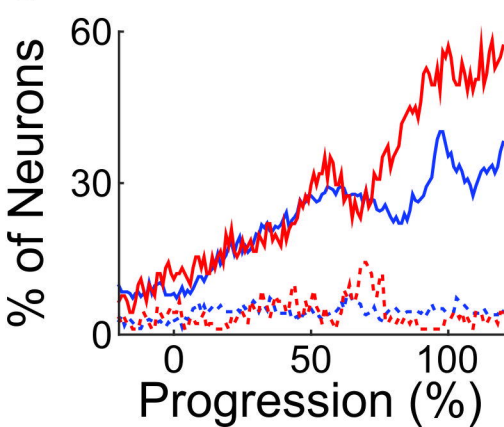


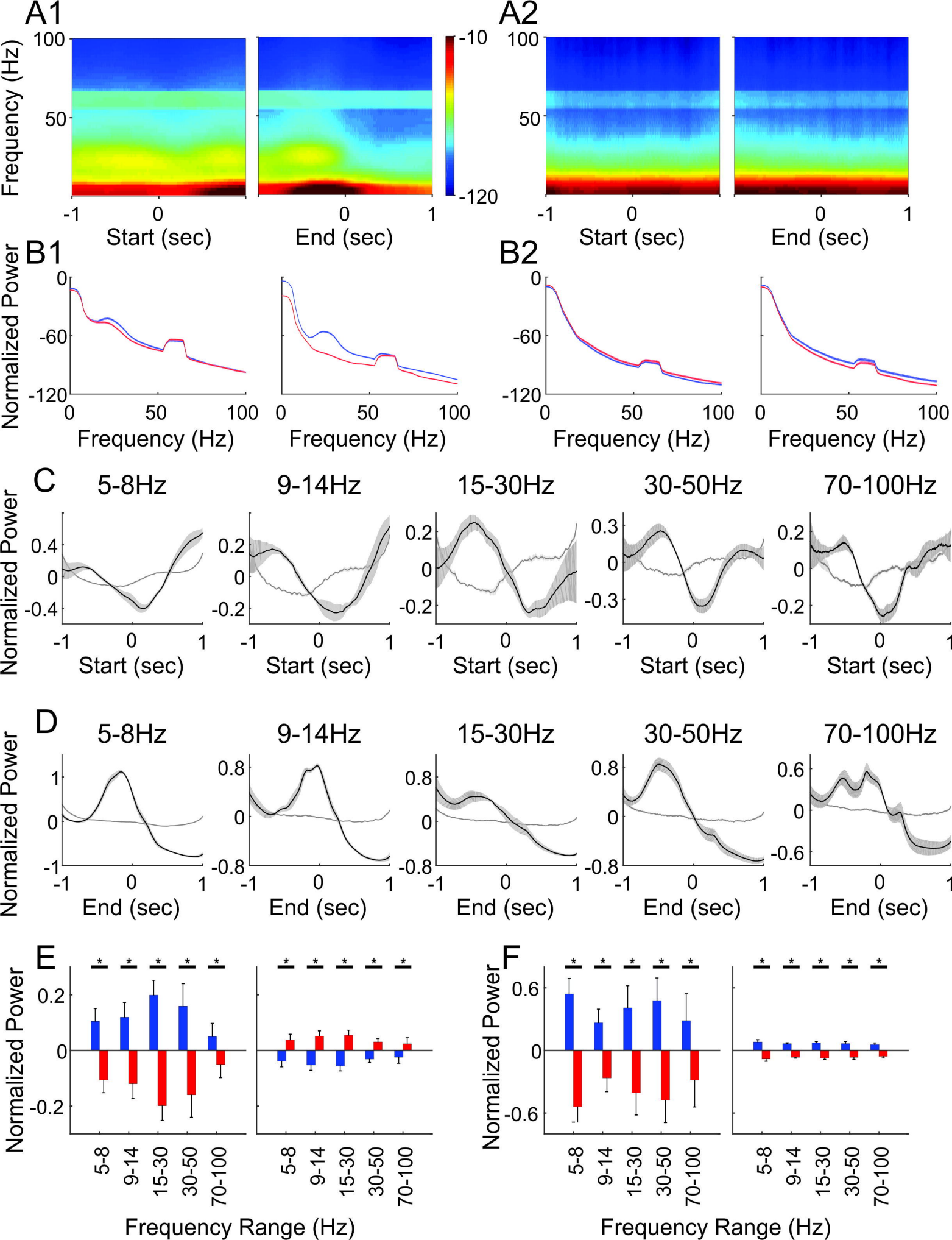
A

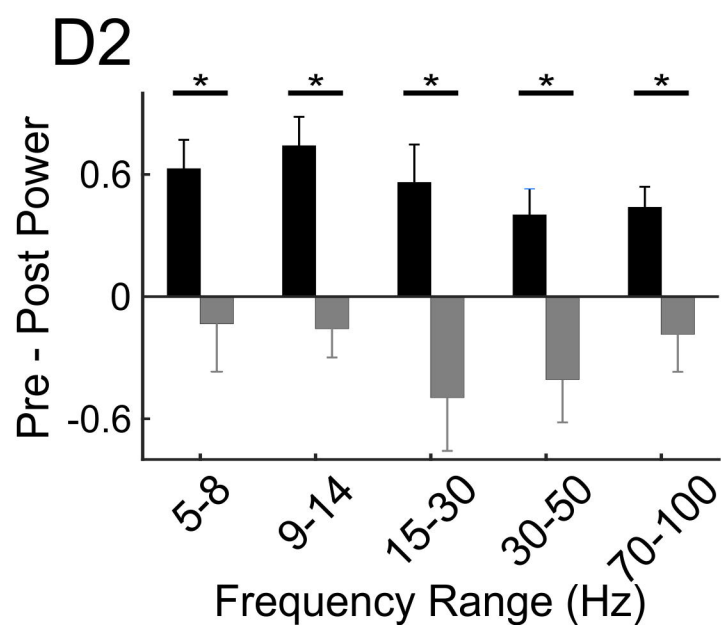
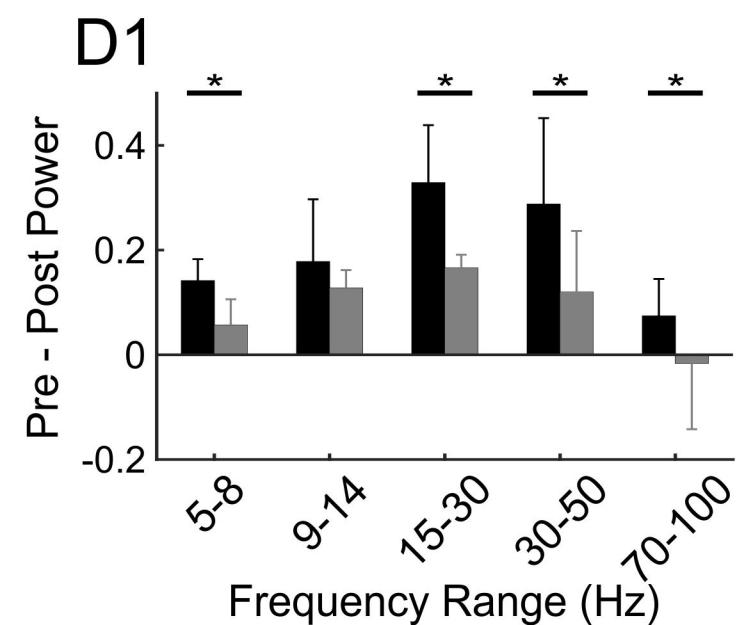
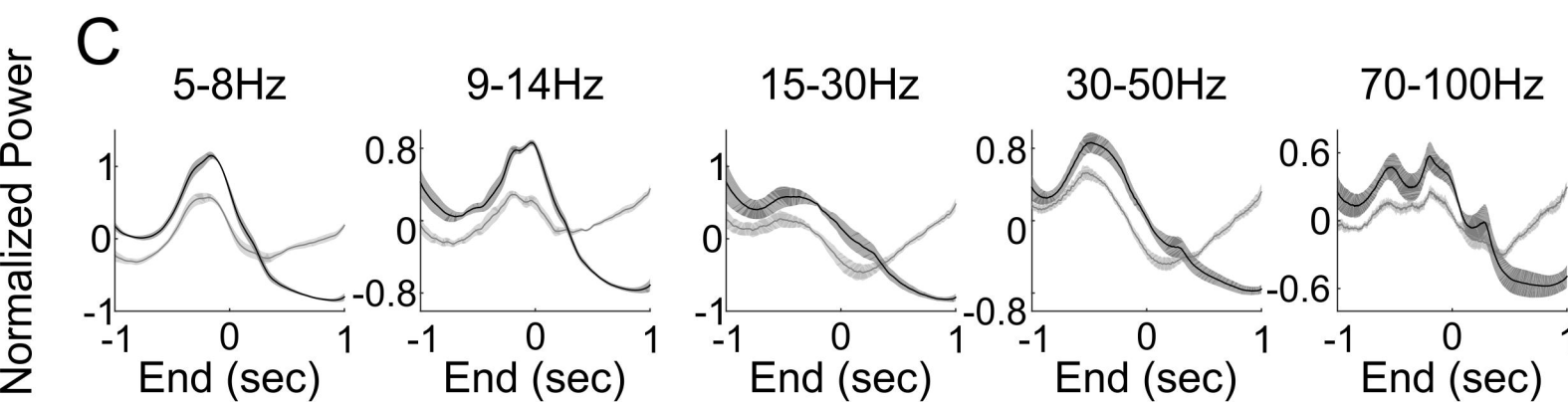
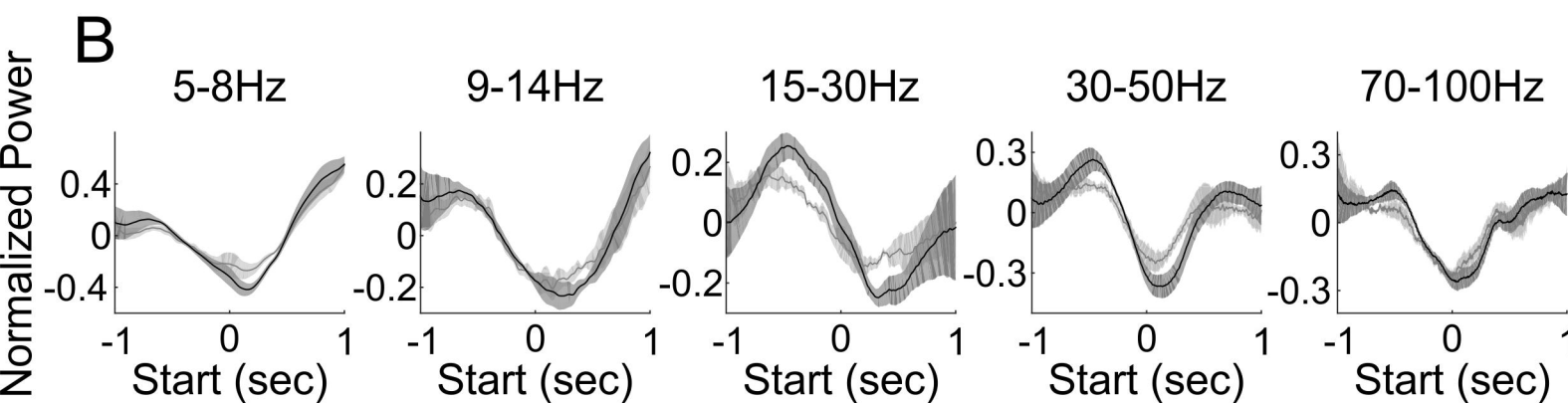
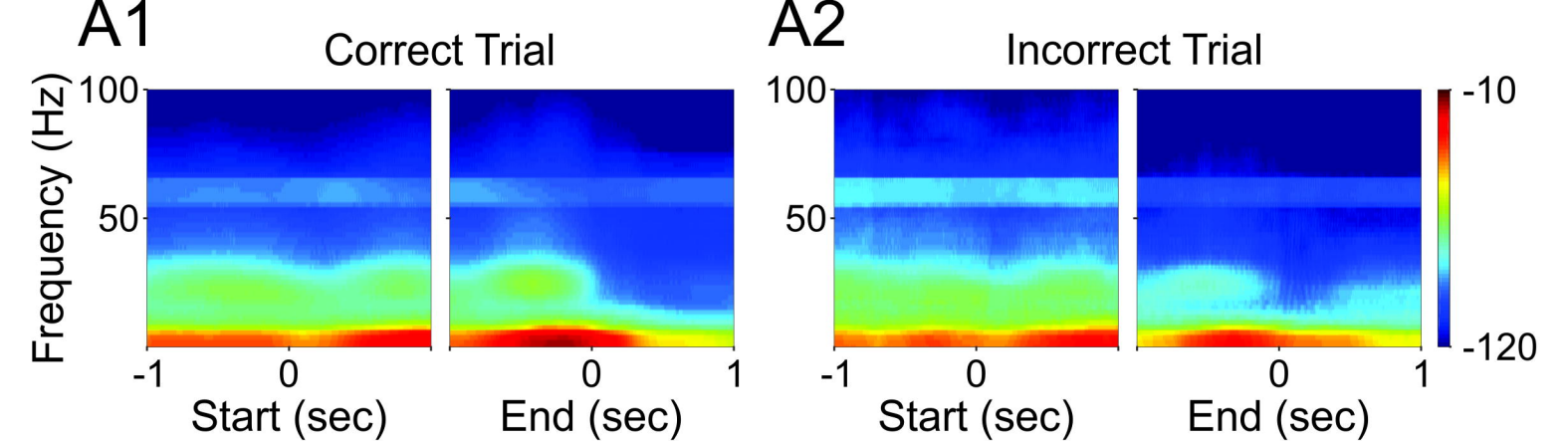
Normalized
Spike Rate

**B**

Normalized
Spike Rate

**C1****C2****D**

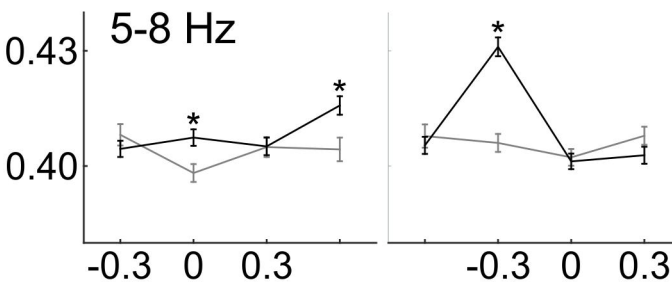




A

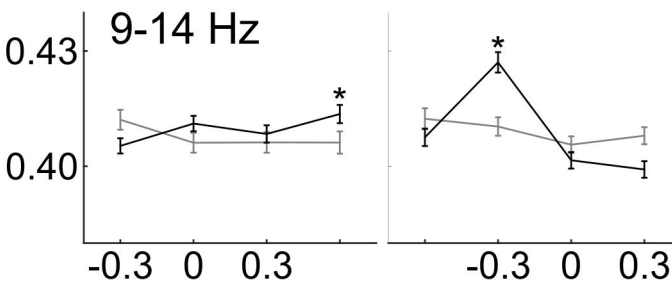
Coherence

5-8 Hz

**B**

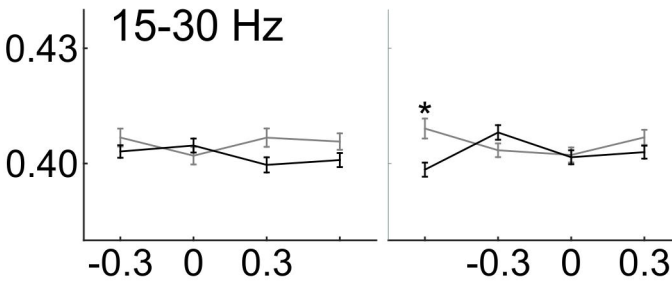
Coherence

9-14 Hz

**C**

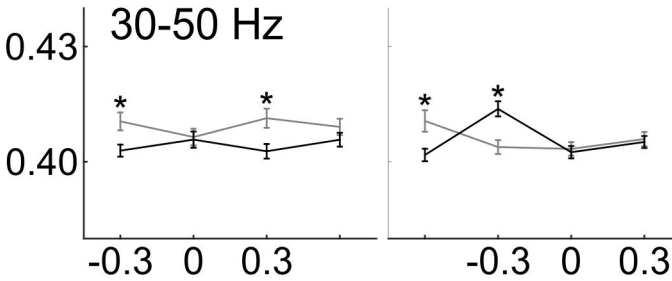
Coherence

15-30 Hz

**D**

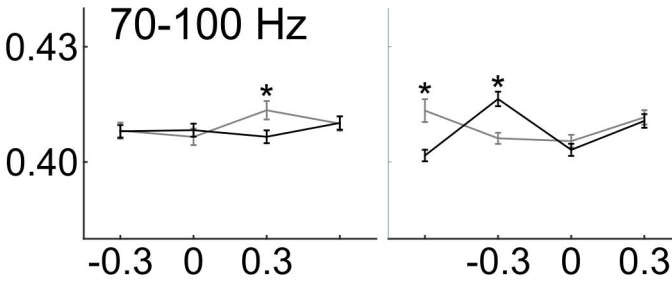
Coherence

30-50 Hz

**E**

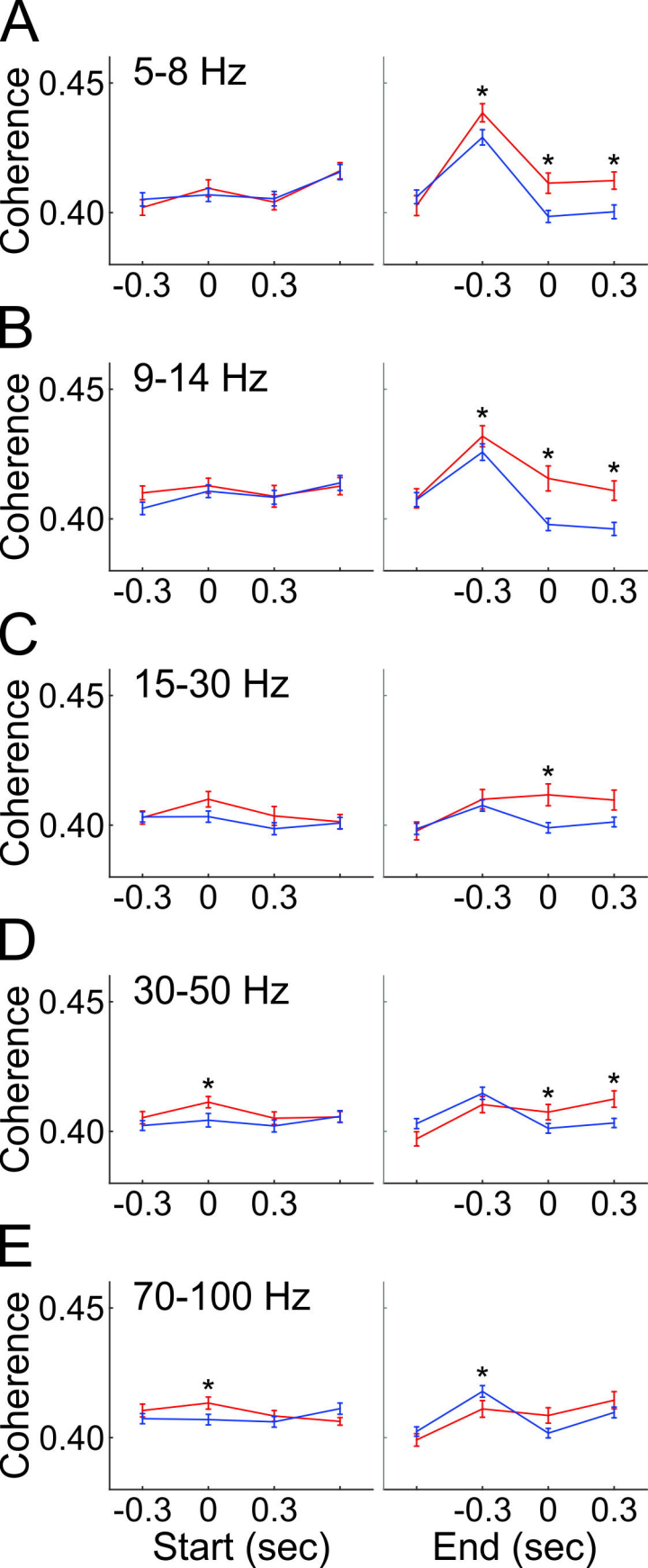
Coherence

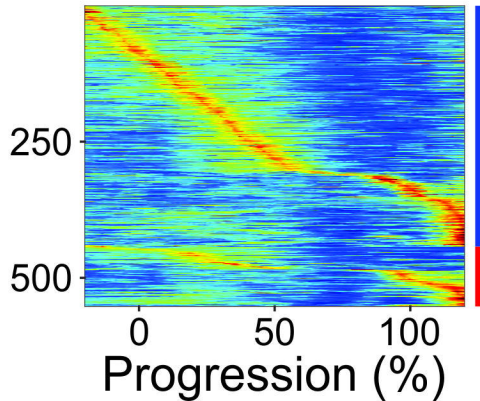
70-100 Hz



Start (sec)

End (sec)



A**Neurons****B****z-score**